Magnetoacoustic quantum oscillations in beryllium*

Robert W. Reed and E. F. Vozenilek†
Department of Physics, The Pennsylvania State University, University Park, Pennsylvania 16802
(Received 18 August 1975; revised manuscript received 11 November 1975)

Magnetoacoustic quantum oscillations have been observed in the absorption of ultrasound in single crystals of Be. The measurements were made with sound frequencies from 0.2 to 1.9 GHz for magnetic fields up to 100 kOe. Extremal cross-sectional areas of the Be Fermi surface have been determined. Quantum oscillation attributed to magnetic breakdown orbits between the "cigar" and "coronet" pieces of the Fermi surface have been observed. Internal magnetization owing to the de Haas–van Alphen effect, caused frequency modulation of the high-frequency magnetic-breakdown-induced quantum oscillations. Several anomalies in the nature of the magnetic-breakdown quantum oscillations are reported.

I. INTRODUCTION

The Fermi surface (FS) of Be has been studied experimentally by a number of investigators using the de Haas–van Alphen (dHvA) effect,[1–3] quantum oscillations in the magnetoresistance,[4–6] sound-velocity quantum oscillations,[7] and both magnetoacoustic geometric oscillations[8,9] and magnetoacoustic quantum oscillations.[9,10]

We report here the results of a series of measurements of the magnetoacoustic quantum oscillations (MAQO's) in Be at sonic frequencies up to 1.9 GHz. Most of the measurements were made with longitudinal sound waves, but a limited number of observations were made with shear waves of random polarization with respect to the crystal axes.[9,10] The measurements were carried out in magnetic fields up to 100 kOe.

The present work gives experimental extremal cross sections of the Be FS in agreement with those determined by other investigators.[1,3] Magnetic-breakdown-induced areas, not previously reported, have been identified. Unexplained anomalies in the nature of the MAQO's associated with the magnetic-breakdown orbits were observed.

II. THEORY

Magnetoacoustic quantum oscillations

Quantum oscillations in the sound attenuation are related to changes in the density of states at the FS as a function of magnetic field. Only electrons within k_BT of the Fermi surface can absorb energy from the sound wave. The electronic mean free path l and the sonic wave vector $\vec{q}$ limit the width of the effective zone of k_z on the FS for phonon absorption by electrons.[11] Three ranges of electronic scattering are found to yield qualitatively different results due to these different zone widths. These are $q_zl \leq 0.7$, $\omega\tau \ll 1$; $q_zl \geq 0.7$, $\omega\tau < 1$; and $q_zl \gg 1$, $\omega\tau > 1$, where q_z is the sound wave-vector component along the direction of the magnetic induction $\vec{B}$, ω is the phonon angular frequency, and τ is the mean electronic scattering time.[11,12] These three regions are referred to as (i) the dHvA region; (ii) the intermediate region, and (iii) the giant quantum-oscillation region, respectively. As ql changes from $ql < 0.7$ to $ql \gg 1$ the character of the observed MAQO's changes from essentially sinusoidal to large amplitude, sharp (δ function) spikes[12] as the region over which the integration of the contribution to the attenuation changes from the entire FS to an infinitesimally small δk_z.[11,12] The areas of extremal cross section obtained from a measurement of the $1/B$ period R of a MAQO are given by the relation

$$1/R = f_G(A) = (\hbar c/2\pi e)A(k_z) \ . \tag{1}$$

Here $f_G(A)$ is the MAQO frequency in G for the area $A(k_z)$. The areas determined from the MAQO's are generally the same areas as obtained by the dHvA effect. (For the special case when $\vec{q}$ is nearly perpendicualr to $\vec{B}$ and $ql \gg 1$ with $\omega\tau > 1$ nonextremal areas may be observed.)

For the dHvA and intermediate regions an expression for the magnetoacoustic ultrasonic attenuation coefficient $\Gamma_j(q,\ l,\ B)$ for the jth extremal cross section of the FS, is[11]

$$\Gamma_j(\vec{q}, l, B) = \Gamma_j(\vec{q}, l, B \to 0) \times \left[1 + G(B)\sum_{S=1}^{\infty} \exp\left(\frac{-S\pi}{\omega_{cj}^{*}\tau_j}\right) \times \frac{S^{1/2}\cos[2\pi S f_G(A_j)/B - 2\pi S\psi - \frac{1}{4}\pi]}{\sinh(2\pi^2 S k_B T/\hbar\omega_{cj}^{*})}\right], \tag{2}$$

where

$$G(B) = \frac{4k_B T m_{cj}^{*} V}{\rho_j \hbar (A_j'')^{1/2}}\left(\frac{\pi c}{e\hbar B}\right)^{1/2} . \tag{3}$$

The zero-field attenuation $\Gamma_j(\vec{q},\ l,\ B \to 0)$ is given, for example by Pippard.[13] The oscillatory term has a fundamental frequency $f_G(A_j)$. The phase factor ψ is generally unknown, but is $\frac{1}{2}$ for free electrons. The factor A_j'' is a FS curvature fac-

tor given by

$$A_j'' = \left(\frac{\partial^2 A_j}{\partial k_z^2}\right)_{E_F, k_{zj}} . \quad (4)$$

V is the specimen volume, T is the temperature, and k_B is the Boltzmann constant. The density of states $\rho_j(E_F, \vec{q}, l, \vec{k}_z)$ is the density of those states at the FS allowed to absorb a sound phonon. If $q_z l > 0.7$, ρ_j is proportional to $(q_z l)^{-1}$, but is independent of $q_z l$ if $q_z l \leq 0.7$. $\omega_{cj}^* \equiv eB/cm_{cj}^*$, where m_{cj}^* is the average cyclotron mass on the orbit in the plane of A_j. The relaxation time τ_j is an average for the orbit about A_j and is related to the Dingle temperature T_D by $T_D \equiv \hbar/2\pi k_B \tau_j$.

Equations (2) and (3) are given in terms of the magnetic induction $\vec{B}$ rather than the magnetic field intensity $\vec{H}$. $\vec{H}$ is the experimentally measured quantity, resulting in MAQO's that are recorded as a function of $1/H$.

Magnetic interaction effects

Be is known to exhibit strong nonlinear magnetization effects.[2,4] In this case, the magnetization $M(B)$ is not correctly given by the Lifshitz-Kosevich (LK) theory which assumes noninteracting electrons,[14] but must be described by a modified Lifshitz-Kosevich equation obtained by replacing H with $B = (H + 4\pi M)$.[2] The oscillatory part of $M(B)$ (the dHvA effect) is determined from the implicit relation

$$M(B) = \sum_{p=1}^{\infty} A_p' \sin\left(\frac{2\pi p f_G}{H + 4\pi M(B)}\right) \quad (5)$$

and A_p' is an amplitude factor varying slowly with B and is not in general equal to A_p of the Lifshitz-Kosevich theory.[14] dHvA measurements of the oscillatory magnetization as a function of H are found to result in distorted wave shapes due to the internal electronic contribution to the magnetization implied by Eq. (5). Equation (5) represents $M(B)$ when the electronic interaction effects are primarily due to a single extremal cross-sectional area described by f_G. For the general case, several such areas will contribute to $M(B)$, further complicating the situation. When B has several oscillatory components (one for each extremal cross section of the Fermi surface), the values of f_G, that are observed as a function of H, will be frequency modulated, and will themselves oscillate about the actual value.

For MAQO's there is no implicit relation similar to Eq. (5) for $\Gamma(B)$. Generally, one treats the "B-H" effect for MAQO's as if the value of B in Eq. (2) is determined by Eq. (5) with the tacit assumption that electrons contributing to $\Gamma(B)$ are independent of those contribution to $M(B)$. Amplitude and frequency modulation of the MAQO's will result from the "B-H" effect, but the wave shapes may differ significantly from the dHvA wave shapes arising from the vicinity of the same external orbits.

In Be the B-H effect can be sufficiently large that free-energy considerations favor the formation of magnetic domains for certain values of applied H.[2] For Be the domain formation occurs because of a very large contribution to $M(B)$ by electrons on the "hip" orbits of the "cigar" portion of the FS.[4] These orbits are designated as α^2 following the notation of TEGS.[3] At values of H for which domains exist, there are disallowed values of B, of width δB, that occur periodically with the frequency (in G) $f_G(\alpha^2)$. The magnetic interaction effects are observed in Be when $\vec{H}$ lies within 45° of the [0001] crystalline direction, where the α^2 orbit dominates the magnetization. In this angular range, electrons on the "waist" orbit (α^1) of the cigar experience the discontinuous magnetization due to α^2, and a distinct "notching" effect is observed in quantum oscillations in the magnetoresistance,[4] sound velocity,[7] and magnetoacoustic attenuation.[10] This notching effect varies with a difference frequency $\Delta f_G = f_G(\alpha^2) - f_G(\alpha^1)$ and is most pronounced at fields $\lesssim 40$ kOe, since the spacing of the α^1 oscillations is $B^2/f_G(\alpha^1)$, whereas the domain region δB, is proportional to H. This notching is not observed (nor is it expected) with the dHvA effect.[2,4]

Magnetic breakdown

When two sheets of the FS in different Brillouin zones are separated by a small energy gap E_g, there exists a finite probability that electrons will tunnel the gap between the separated sheets. The probability for tunneling increases with increasing magnetic field. Electron orbits which are normally confined to one sheet of the FS will, for large tunneling probabilities, be changed to more-nearly-free-electron-like orbits with orbit segments on both parts of the FS.[15]

The electron tunneling probability P for a single approach to the zone boundary is given by

$$P = \exp(-H_0/H) , \quad (6)$$

where H_0 is a parameter (called the breakdown field) defined as

$$H_0 \equiv \frac{\pi}{4} \frac{cE_g^2}{e\hbar |V_x V_y|} \simeq K \frac{m^* c E_g^2}{\hbar e E_F} . \quad (7)$$

The velocities V_x and V_y are components of the Fermi velocity perpendicular to $\vec{H}$, with V_x parallel to the Bragg reflection planes responsible for the gap and V_y perpendicular to these planes. K is a constant, and is usually taken to be of order one, dependent on the FS geometry. A comprehensive discussion of magnetic-breakdown (MB) effects has been given in a review article by Stark and Falicov.[15]

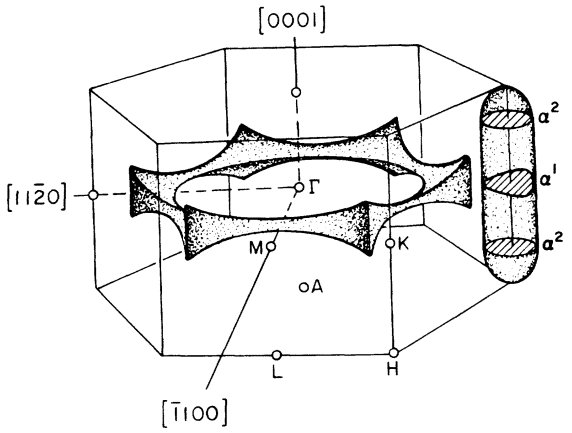

FIG. 1. First Brillouin zone and Fermi surface for Be. The "coronet" is a hole surface in the second Brillouin zone and the "cigars" are electron surfaces in the third zone.

III. FERMI SURFACE OF Be

Figure 1 shows the FS of Be along with the first Brillouin zone. The FS consists of a second zone hole surface called the coronet and six equivalent third zone, electron surfaces which combine to form two "cigars" per coronet. Several theoretical calculations have been made of the FS of Be.[3,16–18] The semiempirical nonlocal pseudopotential model of TEGS[3] gives the best agreement with the available experimental data.

The cross section of the cigar in the basal plane is approximately triangular in shape, and has a vertex of the triangle adjacent to a lobe of the coronet. This midsection α^1 of the cigar in the ΓKM plane, Fig. 1, is the waist and it is characterized by a cross-sectional area that is 3% smaller than cross section α^2 called hips, which are displaced up or down by $\sim\frac{1}{3}$ of the distance KH. The hip cross sections are believed to be more nearly circular in shape. The energy gap between the cigar and coronet is small in the basal plane and MB can occur when the applied $\vec{H}$ is along the [0001] direction (i.e., the electron orbits are parallel to the basal plane).

IV. EXPERIMENTAL METHODS AND PROCEDURES

Measurements of the attenuation of ultrasound in the frequency range of 0.2–1.9 GHz were made as a function of magnetic field from 1 to 100 kOe. The ultrasonic apparatus has been described elsewhere.[19,20] The measurements were made in the temperature range of 1.0–4.2 K.

The magnetic field was supplied by either of two superconducting solenoids. A 10.2-cm-bore 75-kOe solenoid has been described in conjunction with recently reported magnetoacoustic geometric oscillations in Be.[8] In addition to the 75-kOe solenoid, a 100-kOe solenoid with a 6.4-cm bore and 5 parts in 10^4 uniformity over a 2-cm diameter spherical volume (DSV) was used. The 100-kOe solenoid was assembled by placing a Nb_3Sn insert in the bore of the 75-kOe NbTi alloy solenoid and using a series electrical connection. The field in the 100-kOe solenoid was determined using a calibrated (0.1%) Cu magnetoresistance probe. A $1/H$-vs-t sweep unit was used with 75-kOe solenoid. (The hysteresis of the Nb_3Sn insert made the use of this $1/H$ sweep unit impractical with the 100-kOe solenoid.)

Sonic attenuation versus magnetic-field data were recorded on an x-y chart recorder and a strip-chart recorder. The data were also digitized and recorded on punched paper tape. The digital data were fast Fourier analyzed by use of standard computer scientific subroutines. The Fourier analysis typically used 512 or 1024 points. The magnetic-field digital data were recorded to five digits and sonic echo heights to three digits. Be specimens of two purities were employed. The highest-purity Nuclear Metals Inc. (NM) specimens are the same specimens used for the geometric oscillation experiments previously reported.[8] In addition to the high-purity specimens, a large less-pure single-crystal cube 1.1 cm on the side was obtained from The Franklin Institute (FI). The sides of the cube had faces perpendicular to the [0001], [11$\bar{2}$0], and [10$\bar{1}$0] crystal directions. The residual resistance ratio of the FI material was about 90. The NM specimens were too small for reliable resistance ratio measurements but the observation of ~40 geometric-type magnetoacoustic oscillations in one of these specimens showed their excellent purity and crystalline order. CdS vapor-deposited transducers were used on all the Be specimens.

The sample holder[9] for these measurements allowed the samples to be rotated in the magnetic field over a range of ~130°; the rotation axis was perpendicular to the direction of $\vec{H}$. The direction of the sound wave vector $\vec{q}$ was fixed perpendicular to the rotation axis. It was possible to work over a range of sample orientations that included $\vec{q} \parallel \vec{H}$ and $\vec{q} \perp \vec{H}$. The position of $\vec{H}$ in the sample was repeatable to ~0.2°.

V. EXPERIMENTAL RESULTS

Cross-sectional areas

MAQO's were observed with both the FI and NM Be specimens. The area data from the two Be materials were in complete agreement and no distinction will be made between the two sources of data. The data, shown in Fig. 2, are given in terms of the magnetic frequency $f_G(A_j)$ for extremal cross sections A_j [see Eq. (2)]. The relation between the area A_j, in atomic units (a.u.$^{-2}$)

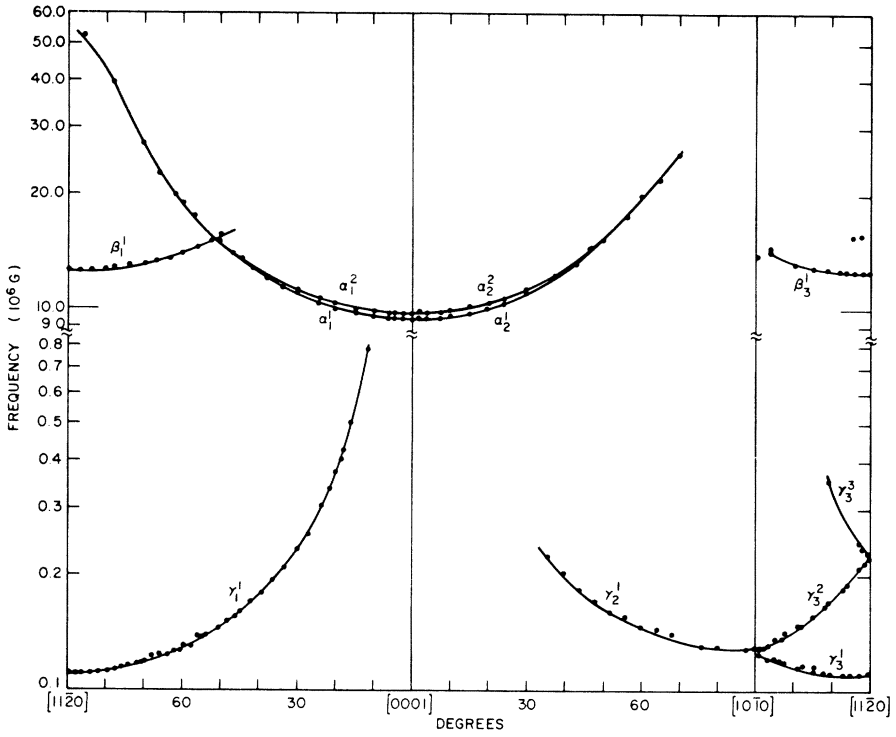

FIG. 2. Semilog plot of all observed quantum oscillations for extremal cross-sectional areas of the Be Fermi surface, excluding magnetic breakdown orbits.

and $f_G(A_j)$ in units of gauss (G) is

$$A_j = 2.673\times 10^{-9} f_G(A_j) \ . \qquad (8)$$

Following the convention of TEGS, Greek letters are used to refer to the FS cross sections responsible for a particular $f_G(A_j)$. Cigar orbits are designated by α, orbits about the thin necks of the coronet by γ, and orbits about the lobes of the coronet by β (see Fig. 3). A subscript defines the planes in which $\vec{H}$ lies (1 for $\{10\bar{1}0\}$, 2 for $\{11\bar{2}0\}$, and 3 for $\{0001\}$). When two or more oscillations arise from a given portion of the FS these are designated by superscripts (e.g., α^1 and α^2 as described above for the waist and hips of the cigar). The β and γ cross sections of the coronet in the basal plane with $\vec{H}$ 15° from $[10\bar{1}0]$ are shown in Fig. 3.

All of the data presented in Fig. 2 were obtained by fast Fourier analysis of the digitally recorded data. The data were obtained with the 75-kOe magnet which was calibrated using proton NMR to give values of H to better than 0.1%. The resulting areas are believed to be accurate to better than ±0.5%. They are in excellent agreement with the dHvA data given by TEGS.[3] It is observed that our magnetoacoustic data for the β cross sections and the higher-frequency α orbits (near $[10\bar{1}0]$ and $[11\bar{2}0]$) are not as complete as those given by TEGS. Table I compares our experimental data for selected cross sections with both the experimental and theoretical values listed by TEGS.

The area of the inner coronet orbit, designated λ^1 by TEGS, in the basal plane was not observed by TEGS,[3] nor was it observed in this work. Magnetoacoustic oscillations data[8] recently reported, however, suggest a smaller area more consistent with the dHvA data of Watts[1] for this orbit than that calculated by TEGS, which is 3.4% larger than the experimental value. The geometric oscillation data also suggest a smaller Γk coronet distance, which would affect calculations of the outer coronet area, designated λ^2 by TEGS.[3] (The orbits λ^1 and λ^2 are the inner and outer circum-

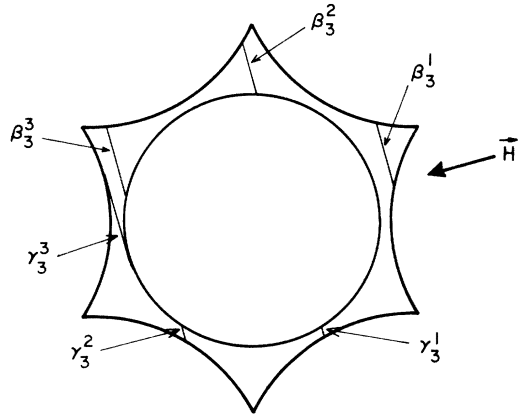

FIG. 3. Coronet cross sections in the basal plane showing the positions of the β_3 and γ_3 orbits when $\vec{H}$ is 15° from the $[10\bar{1}0]$ direction.

TABLE I. Observed quantum oscillation frequencies, compared to the results of TEGS (Ref. 3). (Frequencies are given in units of 10^6 G.)

Fermi surface cross section	Direction of $\vec{H}$	Quantum oscillation frequency (present experiment)	TEGS dHvA frequency	
			Experimental	Theory
Cigar				
α^1	[0001]	9.42	9.42	9.48
α^2	[0001]	9.72	9.72	9.75
α_2^2	50° from [0001]	14.8	14.90	14.92
Coronet				
γ_1^1	$[11\bar{2}0]$	0.111	0.110	0.1097
γ_1^1	11.4° from $[11\bar{2}0]$	0.112	0.112	0.1119
γ_1^1	19.9° from $[11\bar{2}0]$	0.117	0.116	0.1167
γ_1^1	29.4° from $[11\bar{2}0]$	0.128	0.127	0.1262
γ_1^1	35.5° from $[11\bar{2}0]$	0.138	0.138	0.1353
γ_1^1	39.4° from $[11\bar{2}0]$	0.146	0.146	0.1428
γ_1^1	78.4° from $[11\bar{2}0]$	0.776	not given	not given
γ_2^1	$[10\bar{1}0]$	0.128	0.127	0.1270
β_1^1	$[11\bar{2}0]$	12.4	12.4	12.41

ferences of the coronet shown in Fig. 3.)

Magnetic-breakdown quantum oscillations

Several authors[4–6] using magnetoresistance measurements have reported that MB takes place between hole and electron orbits on the coronet and on the cigar, respectively, in the basal plane (i.e., for $\vec{H} \parallel [0001]$). The magnetoresistance measurements indirectly suggest MB by observing where the magnetoresistance changes from the low-field quadratic dependence on H to a saturation of the magnetoresistance. No direct observations of the new electron-hole orbits created by the MB have been reported for Be. Observations of such areas have been made in other *hcp* metals such as Mg.[15,21] The pseudopotential model of TEGS yields a value of $H_0 = 120$ kOe for magnetic breakdown in the basal plane.[3]

Figure 4 shows the kinds of areas involving MB in the basal plane that could be expected to give rise to quantum oscillations. Measurements in the 85- to 100-kOe range have given MAQO's which we attribute to the areas A and $A + \alpha^1$. Figure 5 shows characteristic raw data near 100 kOe. This figure shows one period of the α^2 oscillation and several superposed high-frequency MB oscillations. The MB oscillations were easily observed over more than 15 periods of the slow (α^2) oscillations. Fourier analysis of the slow oscillations showed contributions from both α^1 and α^2 orbits with the α^2 MAQO amplitude being ~ 3–4 times larger. The nodes in the MB oscillations

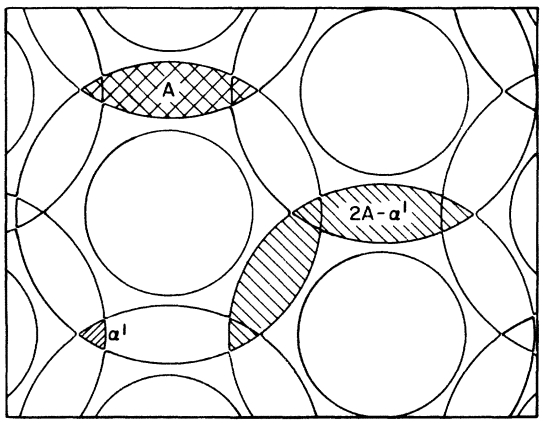

FIG. 4. Magnetic breakdown orbits A and $2A - \alpha^1$ in the basal plane. $\vec{H}$ is along the [0001] axis.

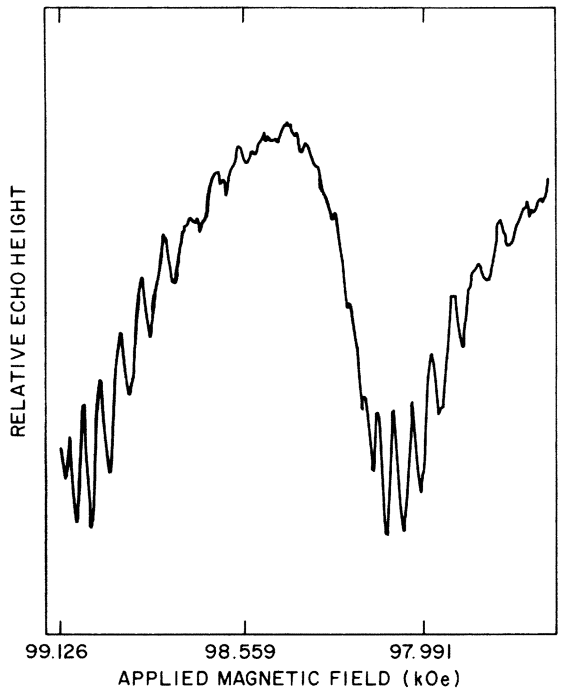

FIG. 5. Magnetic-breakdown quantum oscillations. The breakdown oscillations appear superposed on the large α^2 oscillations, for which one period is shown. The high-frequency oscillations are believed to be from areas A and $A+\alpha^1$ of Fig. 4.

(one occurs at ~98.5 kOe in Fig. 5) were observed to move relative to the peaks of the slow oscillations. Thus since the slow oscillation is dominated by α^2 it was concluded that the difference frequency causing the nodes in the high-frequency MB oscillations was most likely equal to $f_G(\alpha^1)$. This implies that quantum oscillations from two MB orbits differing in size by α^1, are beating together to produce the observed beat. Such a combination would be area A and area $A+\alpha^1$ (the electrons make an extra trip around one cigar waist) of Fig. 4. Careful examination of Fig. 5 also shows that the periods of the high-frequency oscillations are not of uniform size.

Fourier analysis of data similar to Fig. 5 over the range of 93–100 kOe gives a spectrum of frequencies characteristic of a frequency-modulated signal.[22] A typical spectrum is shown in Fig. 6. This frequency modulation arises from recording the MAQO's as a function of H rather than B. Since B is related to H by[4]

$$B(H) = H + 4\pi(1-L)M(B)\ , \tag{9}$$

where L is the demagnetization factor, and since $M(B)$ is a periodic function of B due to the B-H effect, the $B(H)$ field varies periodically about the value of the applied H. The amplitude of the modulation of $B(H)$ by $M(B)$ is determined by the amplitude of the dHvA oscillations. In Be the dHvA effect is large for the α^1 and α^2 orbits, with the electrons on the α^2 orbits dominating $M(B)$.[2] It must be stressed that both sets of oscillations in Fig. 5 are MAQO's that are phase modulated by the dHvA oscillations. The amplitude and frequency of the MAQO's are not simply related to the dHvA oscillations modulating them. The modulating dHvA frequency will be a weighted average of $f_G(\alpha^1)$ and $f_G(\alpha^2)$ with a net amplitude and wave shape that results from a self-consistent solution of an equation similar to Eq. (5) but summed over $f_G(\alpha^1)$ and $f_G(\alpha^2)$. This modulation frequency will be the difference frequency separating the FM spectral terms or peaks of Fig. 6. Unless the modulation amplitude is known, one cannot determine which of the peaks of Fig. 6 represent the physically meaningful values for f_G although the spectrum must include them.

Using the λ^2 outer coronet area calculated by TEGS,[3] the area α^1, and the dimensions of the Brillouin zone, the expected values for the frequencies due to areas A and $A+\alpha^1$ are calculated to be $f_G(A) = 1.42\times10^8$ G and $f_G(A+\alpha^1) = 1.51\times10^8$ G. These values are within 3% of the prominent lines at 1.455 and 1.555×10^8 G shown in Fig. 6. (For a different pair of lines in Fig. 6 to be the correct values for these orbits would require the TEGS value for the λ^2 coronet area to be in error by ~6% or multiples thereof.) Becausethe modulation frequency is very nearly equal to the expected difference frequency $f_G(A+\alpha^1) - f_G(A)$, the Fourier spectrum cannot be used to prove the existence of more than one breakdown orbit although it is apparent that two orbits are beating together

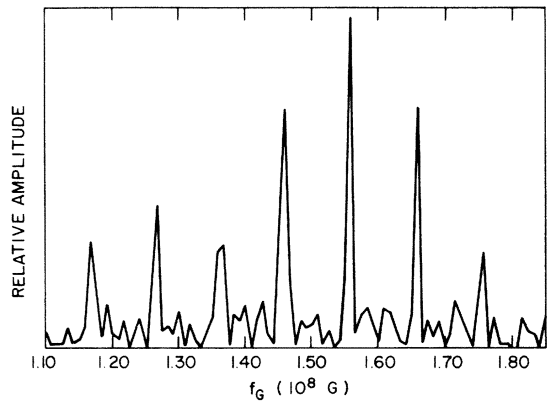

FIG. 6. Fourier spectrum of low-frequency magnetic-breakdown quantum oscillations. The data were taken from 89 to 100 kOe for shear waves of random polarization at a frequency of 1.2 GHz. Here $\vec{g} \parallel [11\bar{2}0]$ and $\vec{H} \parallel [0001]$. This is a 1024-point transform with 84 of the 512 components used to generate this plot. It is proposed that these data contain the values of f_G for areas A and $A+\alpha^1$ of Fig. 4.

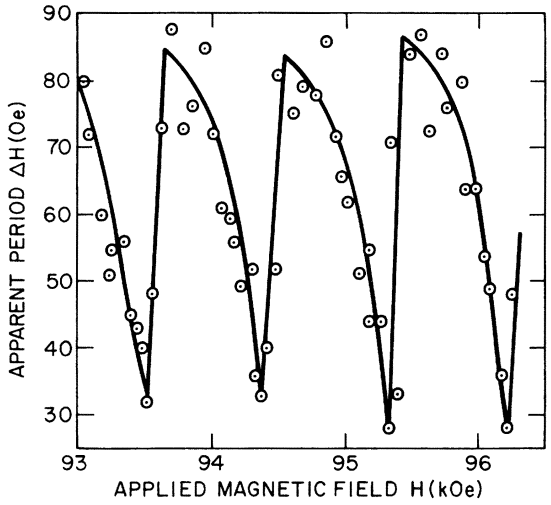

FIG. 7. Plot of individual ΔH periods for magnetic-breakdown data. A portion of the same data used to generate Fig. 6, was used to generate this plot. The f_G values, corresponding to the ΔH periods shown, range from about 1.1×10^8 to 3.3×10^8 G within an average value of 1.465×10^8 G for $93 \leq H \leq 100$ kOe.

as evidenced in Fig. 5.

Figure 7 shows a plot of the individual periods in ΔH for 54 of the MB oscillations used to obtain Fig. 6. These data were read by hand from a calibrated strip chart recording. The ΔH periods of Fig. 7 correspond to a range of about 1.1 to 3.3×10^8 G for f_G. The 3-to-1 range of frequencies occurs with a periodicity approximately equal to one of the α frequencies; i.e., the modulation frequency due to the magnetic interaction is $f_G(\alpha)$. The average frequency for the range $93 \leq H \leq 100$

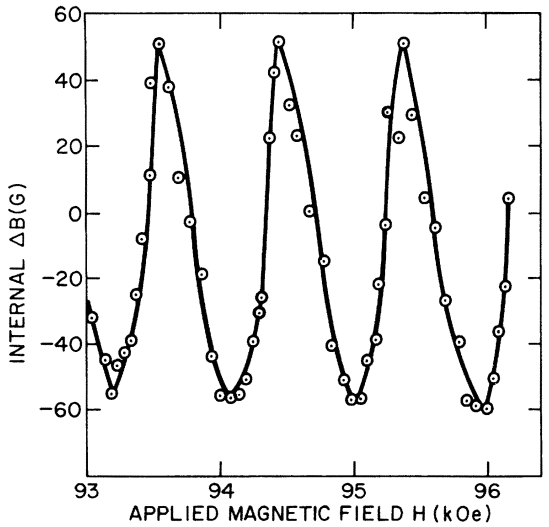

FIG. 8. Plot of internal ΔB required to make data of Fig. 7 all have same value of $f_G = 1.465\times10^8$ G (i.e., B(internal) = H(applied) + ΔB).

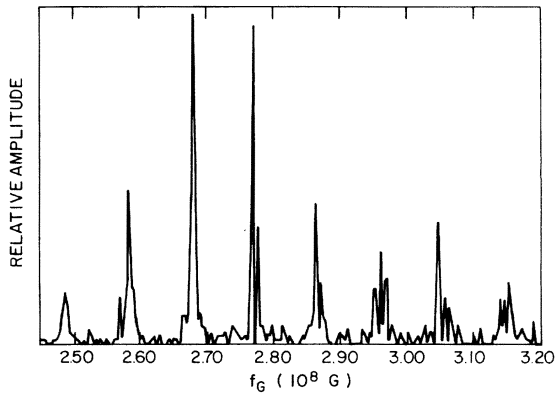

FIG. 9. Fourier spectrum of high-frequency magnetic breakdown quantum oscillations. The data were taken from 59 to 71 kOe using longitudinal sound at 1.20 GHz. Here $\vec{g} \parallel [11\bar{2}0]$ and $\vec{H} \parallel [0001]$. This is a 2048-point transform with 219 of the 1024 components used to generate this plot. It is proposed that these data contain the values of f_G for areas $2A - \alpha^1$ and $2A$ of Fig. 4.

kOe of the data including that of Fig. 7 is $f_G = 1.464\times10^8$ G. If one were to assume that this corresponds to the carrier frequency, the position in B for each oscillation could be calculated and the difference $\Delta B = B_{cal} - B_{expt}$ (= H) obtained for each peak. Figure 8 shows such a plot for the data of Fig. 7. The ΔB values of Fig. 8 are thus equal to $4\pi M(B)$ of the dHvA oscillations responsible for producing the MAQO modulation. $4\pi M(B)$ has a peak value of ~ 50 G at 95 kG and occurs at a dHvA frequency f_G corresponding to $f_G(\alpha^1)$, $f(\alpha^2)$ or some weighted average of these. (Other values of f_G as indicated by Fig. 6 were also tried but the resulting values of ΔB did not maintain a steady base line at $\Delta B = OG$ in Fig. 8.) These values of $4\pi M(B)$ are reasonable in view of Condon's dHvA data taken at 28 kOe which yields an absolute dHvA amplitude for $4\pi M(B)$ of ~ 14 G peak.[2]

MB MAQO's, with f_G values about twice those described above, were recorded with the more uniform 75-kOe magnet. Figure 9 shows a typical Fourier spectrum of these data. The strip chart recordings show obvious beats at $\sim 9.4\times10^6$ G $- f_G(\alpha^1)$, which we attribute to beating oscillations from areas $2A - \alpha^1$ and $2A$. If the peaks of Fig. 9 at 2.78×10^8 and 2.875×10^8 G are assigned to $2A - \alpha^1$ and $2A$, respectively, the resulting value for A is 1.44×10^8 G. This is in good agreement with Fig. 6, which has a peak at 1.455×10^8 G. {Note that splitting of the spectra at 2.78×10^8 G in Fig. 9 could be due to the difference between the FM modulation frequency [$\sim f_G(\alpha^2) = 9.72\times10^6$ G] and the beat frequency between $f_G(2A)$ and $f_G(2A - \alpha^1)$, which is $f_G(\alpha^1) = 9.42\times10^6$ G. The resolution of the data of Fig. 6 was insufficient to observe such splitting.}

From the above considerations we assign the f_G values for the MB areas as follows: (a) $f_G(A) = 1.45\times10^8$ G, (b) $f_G(A+\alpha^1) = 1.55\times10^8$ G, (c) $f_G(2A-\alpha^1) = 2.78\times10^8$ G, and (d) $f_G(2A) = 2.88\times10^8$ G. Our assigned values imply $f_G(A)$ to be $1.45\pm0.01\times10^8$ G, which is about 3% in excess of the estimates obtained from the TEGS calculations.[3] To bring these facts into coincidence would require the TEGS calculated λ^2 coronet area to be too large by about 3%. Estimates of the change in the λ^2 area that would result if the Γk coronet dimension (see Ref. 8, Fig. 6) were corrected to that obtained from geometric oscillations[8] indicate a reduction of ~ (2 to 3)%. This would support our findings in this work. The implications of this change in the coronet, with respect to effects on the shape of the cigar and the magnetic breakdown energy gap are not clear. It is also surprising that the dHvA studies by TEGS[3] did not yield any observation of MB orbits. This is particularly true in light of the fact that they worked at fields up to 60 kOe and had sufficient field uniformity to make a search for oscillations from the large basal plane orbits about the coronet.

Magnetic-breakdown observation anomalies

The high-frequency MB data (from areas $2A$ and $2A-\alpha^1$) were observed at lower values of H than the lower-frequency data (from areas A and $A+\alpha^1$). The fact that high-frequency data could only be obtained with the more uniform 75-kOe magnet and could not be observed with the 100-kOe magnet, even at the same field values, leads us to conclude that the poorer uniformity of field in the 100-kOe solenoid limits the observation of the higher-frequency oscillations. One would expect from Eq. (6) that areas A, $A+\alpha^1$, $2A-\alpha^1$, and $2A$ would be observed with increasing H in this order. Several attempts with the high-uniformity magnet yielded no evidence for MB MAQO's due to orbits A or $A+\alpha^1$ at fields below 60 kOe, where the $f_G(2A-\alpha^1)$ data were already clearly apparent. Since the magnetoresistance data imply that MB commences near $H=20$ kOe,[4,5] the lower-frequency orbits should be observable, in the 50-kOe region. The 75-kOe magnet had more than sufficient uniformity of field to allow the observation of $f_G(A)$ at 40 kOe. These observations were independent of the Be specimens used.

The MB MAQO's reported here have only been observed for $\vec{H}$ lying within $\pm1^\circ$ of the [0001] crystalline direction. This angular dependence is consistent with observations of orbits about the coronet as seen by previous experiments using magnetoacoustic geometric oscillations.[8] The data were all taken with the specimens at 1 K. For temperature above 2 K the MB MAQO's disappeared into the noise. No evidence could be found, for H up to 100 kOe, for MB oscillations for $\vec{q} \parallel [0001] \parallel \vec{H}$. For the case of either $\vec{q} \parallel [11\bar{2}0]$ or $\vec{q} \parallel [10\bar{1}0]$ with $\vec{H} \parallel [0001]$, so that $\vec{q} \perp \vec{H}$, the MB oscillations were very readily observed in either the pure NM specimens or the less pure FI specimens. The MB oscillations were observed with any sonic frequency used, with the amplitude of the MAQO's being approximately proportional to the sonic frequency. The MB oscillations were observed for both longitudinal and shear waves. Most of the shear wave data were taken with random polarizations generated by the CdS transducers on the FI specimens. Similar shear wave results were obtained with a quartz AC cut shear transducer, indium bonded to an NM specimen, with $\vec{\epsilon} \parallel [0001]$ and $\vec{q} \parallel [11\bar{2}0]$. Operation with the quartz transducer (15-MHz fundamental) was restricted to frequencies below 405 MHz by system attenuation. The theory for magnetoacoustic quantum oscillations[13] predicts that for specimens with $ql \gtrsim 1$ the oscillations for $\vec{q} \perp \vec{H}$ should be greatly reduced in amplitude over that of the case for $\vec{q} \parallel \vec{H}$ and $\vec{H}$ along the same crystalline direction as in the $\vec{q} \perp \vec{H}$ case. With the NM specimens it is clear that $ql > 1$, as is evidenced by the observation of magnetoacoustic geometric oscillations in the same specimens.[8] For the case of MAQO's due to the α^1 and α^2 orbits, the theory[13] is consistent with our observations, with $\vec{q} \parallel \vec{H} \parallel [0001]$ clearly giving rise to much larger oscillations than for $\vec{q} \perp \vec{H} \parallel [0001]$ for both longitudinal and shear waves, in both the NM and FI specimens.

The fact that the effects described in the present section were obtained for both the cubic FI specimen and the thin-disk NM specimens reduces the possibility that the effects were caused by the sample-shape-dependent demagnetization factor L of Eq. (9). This factor would be expected to alter the magnetic interaction effect,[2] particularly the wave shape of the dHvA oscillations which are responsible for the observed frequency modulation. Since observations of MB orbits are more often made by use of the dHvA effect, rather than the MAQO effect one might be induced to look at the nature of the MAQO effect for the explanation of the unexpected $\vec{q} \perp \vec{H}$ requirement for observing MB orbits in Be. However, an earlier investigation of Mg by the MAQO effect gave good observation of MB orbits with $\vec{q} \parallel \vec{H}$.[11]

Throughout these investigations of MAQO's, qualitative differences in the data that depend on propagation mode (longitudinal or shear) and on propagation direction have been observed. These were consistent with, and further support an earlier report of these effects.[10]

VI. CONCLUSIONS

Cross-sectional areas of the FS of Be have been measured and are in good agreement with data from the dHvA effect.[3] Magnetoacoustic quantum oscillations due to MB orbits between the "cigar" and "coronet" pieces of the FS have been observed. Such orbits have not been reported by observers using other techniques such as the dHvA effect. Large magnetic interaction effects cause frequency modulation of the MB data and prevent precise assignment of the frequencies resulting from Fourier spectrum analysis of the data to a particular MB orbit. The frequency spectra contain frequencies close to those predicted for such MB orbits by the TEGS[3] pseudopotential model of the FS of Be. The TEGS pseudopotential model erroneously predicts that magnetic breakdown in the basal plane between the cigars and the coronet should take place at $\sim H_0 = 120$ kOe. The present results show that H_0 must be at least as low as 50 kOe. Anomalies in the character of the MB quantum oscillations require further investigation.

ACKNOWLEDGMENTS

The authors are particularly indebted to Professor F. G. Brickwedde for his many helpful suggestions and stimulating discussions throughout the course of the investigation. The help of Alexander Marker III in the recording of data is greatly appreciated.

---

*Supported by the Applied Research Laboratory of The Pennsylvania State University, under contract with the U. S. Naval Sea Systems Command.

†Present address: Corning Glass Works, Sullivan Park, Corning, N. Y. 14870.

[1]B. R. Watts, Proc. R. Soc. Lond. A 282, 521 (1964).

[2]J. H. Condon, Phys. Rev. 145, 526 (1966).

[3]J. H. Tripp, P. M. Everett, W. L. Gordon, and R. W. Stark, Phys. Rev. 180, 669 (1969).

[4]W. A. Reed and J. H. Condon, Phys. Rev. B 1, 3504 (1970).

[5]D. J. Sellmyer, I. S. Goldstein, and B. I. Averbach, Phys. Rev. B 4, 4628 (1971).

[6]W. A. Reed, in *Proceedings of the Eleventh International Conference on Low-Temperature Physics*, edited by J. F. Allen (University of St. Andrews, St. Andrews, Scotland, 1969), p. 1160

[7]L. R. Testardi and J. H. Condon, Phys. Rev. B 1, 3928 (1970).

[8]E. F. Vozenilek and R. W. Reed, Phys. Rev. B 12, 1140 (1975).

[9]E. F. Vozenilek, Ph. D. thesis (The Pennsylvania State University, 1975) (unpublished).

[10]E. F. Vozenilek, R. W. Reed, and F. G. Brickwedde, in 1975 *Ultrasonics Symposium Proceedings*, edited by J. de Klerk (IEEE, New York, 1975), p. 453.

[11]R. W. Reed and F. G. Brickwedde, Phys. Rev. B 3, 1081 (1971).

[12]S. H. Liu and A. M. Toxen, Phys. Rev. 138, A487 (1965).

[13]A. B. Pippard, *The Dynamics of Conduction Electrons* (Gordon and Breach, New York, 1965), p. 120.

[14]A. V. Gold, *Solid State Physics, Vol. I: Electrons in Metals*, edited by J. F. Cochran and R. R. Haering (Gordon and Breach, New York, 1968).

[15]R. W. Stark and L. M. Falicov, *Progress in Low Temperature Physics* (Wiley, New York, 1967), Vol. 5.

[16]T. L. Loucks and P. H. Cutler, Phys. Rev. 133, A819 (1964).

[17]T. L. Loucks, Phys. Rev. 134, A1618 (1964).

[18]J. H. Terrell, Phys. Rev. 149, 526 (1966).

[19]R. W. Reed, D. E. Binnie, and F. G. Brickwedde, J. Acoust. Soc. Am. 51, 910 (1972).

[20]R. W. Reed, J. Acoust. Soc. Am. 56, 886 (1974).

[21]R. W. Stark, Phys. Rev. 162, 589 (1967).

[22]L. B. Arguimbau, *Vacuum-Tube Circuits and Transistors* (Wiley, New York, 1956).